

# Voxel-based dose calculation of radionuclide imaging and therapy for preclinical studies using GEANT4 Monte Carlo simulation

H. Liu<sup>1</sup>, C. Geng<sup>1,2\*</sup>, X. Tang<sup>1,2</sup>, L. Tang<sup>3</sup>, X. Li<sup>3</sup>, P. Xu<sup>1</sup>

<sup>1</sup>Department of Nuclear Science and Technology Nanjing University of Aeronautics and Astronautics, 29 General Road, Jiangning District, Nanjing 211106, China

<sup>2</sup>Key Laboratory of Nuclear Technology Application and Radiation Protection in Astronautics (Nanjing University of Aeronautics and Astronautics), Ministry of Industry and Information Technology, 29 General Road, Jiangning District, Nanjing 211106, China

<sup>3</sup>MITRO Biotech Co., Ltd, Building 8, No.5 Qiande Road, Nanjing 211106, 211106, China

## ABSTRACT

### ► Original article

#### \*Corresponding author:

Changran Geng, Ph.D.,

E-mail: gengchr@nuaa.edu.cn

Received: March 2021

Final revised: August 2021

Accepted: September 2021

Int. J. Radiat. Res., April 2022;  
20(2): 317-322

DOI: 10.52547/ijrr.20.2.9

**Keywords:** Internal dosimetry, radiopharmaceutical, Monte Carlo simulation, MIRD.

**Background:** This study aims to investigate voxel-level dose calculation methods and improve its calculation efficiency in nuclear medicine that can consider animal-specific heterogeneous tissue compositions and radiopharmaceutical biodistributions simultaneously. **Materials and Methods:** The voxelized mouse phantom was constructed from real mouse CT images and simulated using the Monte Carlo GEANT4 code. According to the dynamic PET images of real mouse, the real distribution of radiopharmaceutical activity was set in the Monte Carlo simulation. The sampling method to improve the calculation efficiency was proposed. Two voxel-level dose calculation methods were implemented in this study. The average absorbed dose in vital target organs and the tumor was calculated by the proposed voxel-level dose calculation methods and the traditional MIRD method respectively. The results of the average absorbed dose calculated by the two methods were compared. Based on the voxel-level dose calculation method, the three-dimensional dose distribution in organs and the tumor was obtained and evaluated. **Results:** The relative difference of average absorbed dose between the two voxel-level dose calculation methods was mostly less than 10%. The sampling method proposed to improve calculation efficiency for the voxel-level dose calculation can decrease the calculation time by ~34% with less deviation. **Conclusion:** The results confirmed that the voxel-level dose calculation methods proposed in this study allow for more accurate and efficient assessment of the internal radiation dose.

## INTRODUCTION

Dosimetry is of critical significance for evaluating therapeutic effectiveness and toxicities during clinical and preclinical targeted radionuclide therapy (TRT) (1). Small animals, particularly the mouse, have been increasingly used in preclinical research to develop novel radiopharmaceuticals for treatment and diagnosis of human illness (2). Traditionally, Medical Internal Radiation Dose (MIRD) schema was used to estimate absorbed dose in small animals (3), which was based on organ-level S-values. However, the shortcoming of this approach is that it does not consider patient- or animal-specific tissue and radioactivity distribution (4).

To address the drawback of the organ-level MIRD schema, voxel-based dosimetry methods have been suggested, including the dose point kernel (DPK) and voxel S-value (VSV) (5-8). The VSV requires tabulated S-values for each radioactive nuclide with the

corresponding voxel size. Establishing the database of S-values for various radioactive nuclides with a variety of voxel dimensions has a huge workload, which is yet not available. In addition, another method that can be used for internal radiation dose assessment is Monte Carlo (MC), which is currently considered to be a most accurate method in the field of dose assessment because it simulates the detail transportation process of particles in objects (9, 10). Based on the animal phantoms, specific absorbed fractions, S-values and absorbed doses of several radionuclides have been calculated by the use of MC software, such as EGS, MCNP, GAMOS, GATE, etc. (11-13). However, as is known, long simulation time is the limit for MC method. Thus, shortening the time of Monte Carlo simulation is also a matter of concern (14).

This study aims to explore the GEANT4-based approach to estimate the dose distribution considering animal-specific or patient-specific

heterogeneous tissue compositions and radiopharmaceutical biodistributions simultaneously, and propose a method for improving the calculation efficiency.

## MATERIALS AND METHODS

### Animals

The mouse of 8 weeks old, weighing 17.71 g, implanted with breast cancer cells under its armpits, was used in this study. The license for the use of experimental animals is syxk (Su) 2015-0014 issued on 2015. The breeding conditions were 12 hours light and dark alternation, free drinking and feeding at the MITRO Biotech Co., Ltd. The volume of the tumor in the mouse is about 0.607 cm<sup>3</sup> for this study after two weeks growth. Radiopharmaceutical used in this study was <sup>89</sup>Zr- Her2 Monoclonal antibody targeting breast cancer cells (produced by the MITRO Biotech Co., Ltd). The mouse was scanned by small animal PET/CT scanner (SNPC-103, Pingseng, China) for 10 min at 2 H, 24 H, 72 H, 140 H, 214 H, 336 H and 504 H after intravenous injection (IV) of radiopharmaceutical via its tail vein, as the figure 1 illustrated.

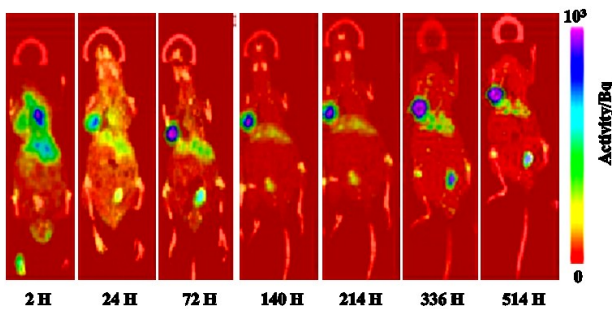


Figure 1. The coronal PET/CT image at various time points after injection of radiopharmaceutical which is the middle slice of all images.

### Activity calculation

All the PET images were reconstructed by the iterative algorithm, which incorporates the correction for attenuation, scatter, and decay. The resolution of reconstructed images is 0.6667×0.6667×0.6 mm<sup>3</sup> and the size of whole image matrix is 150×150×212. The three dimensional activity map in the mouse were acquired according to equation (1):

$$U = m \cdot SV + b \quad (1)$$

Where *m* is Rescale Slope (which is different in each image slice), *SV* is the Pixel intensity Value, *b* is rescale intercept and *U*(Bq) is units of value after conversion<sup>(15)</sup>.

Activities of each organ was estimated by organ segmentation with the segmentation module of 3D Slicer (version 4.2.0), which is an open source software platform for medical image informatics,

image processing, and three-dimensional visualization<sup>(15-17)</sup>.

### Methods to estimate preclinical dosimetry

The preclinical dosimetry was calculated by the Monte Carlo toolkit Geeant4 (version 10.05.p01), which has been widely used for medical dosimetry<sup>(18)</sup>. The physics list used in this research involved "G4DecayPhysics", "G4RadioactiveDecayPhysics" and "G4EmStandardPhysics". The mouse geometry for dose calculation was constructed based on the CT images. Tissues were divided into 25 materials based on the Schneider method, which converts the Hounsfield Unit (HU) value to material density and elemental composition<sup>(15)</sup>. The resolution of the reconstructed geometry is 0.43×0.43×0.6 mm<sup>3</sup>. The number of simulated histories were 1×10<sup>8</sup> in all cases.

In order to consider the realistic activity distributions in organs and tumors during the process of calculating doses with GEANT4, two methods (Method 1 and 2) to estimate preclinical voxel-based dosimetry with PET/CT imaging of the mouse was implemented in this study. Besides, the organ-level dosimetry using MIRD schema (Method 3) was also performed for comparison.

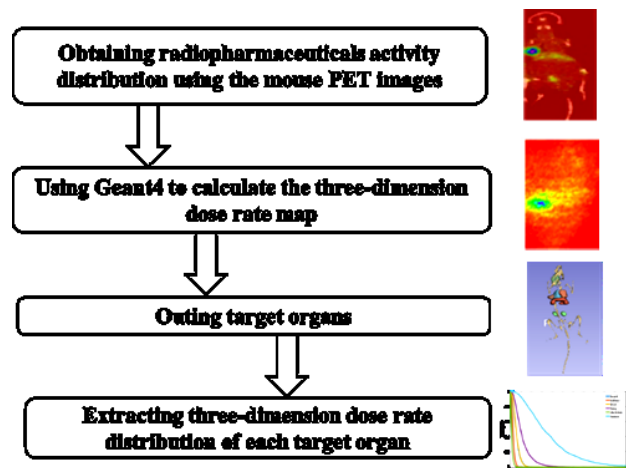


Figure 2. Process of methods estimating preclinical dosimetry at voxel-level.

In the Method 1, the primary particle is sampled with the probability of the radioactivity in each voxel. In this method, the activity value in each voxel was normalized by the total activity in the mouse to obtain the probability of emitting particles at each voxel. The primary particle is distributed uniformly in one specific voxel. With that, the dose deposition of each voxel in the phantom can then be calculated through the Monte Carlo simulation.

Different from method 1, method 2 samples the primary particle uniformly over the whole mouse where the radioactivity existed, however, the primary particle will be attributed with a weight, which is associated with the radioactivity in each voxel. In the Primary Generation class file of GEANT4, the source

was assumed to emit uniformly in the total mouse phantom. Through the particle gun, the probability of emitting a source particle in the sampled voxel was assigned to the particle as the particle weight. The primary particle and its secondary particles shared the same weight. The dose deposition of each voxel in the phantom can then be multiplied the weight to obtain the reasonable dose distribution in voxel level. This method is proposed for shortening the calculation time for the voxel-level dosimetry.

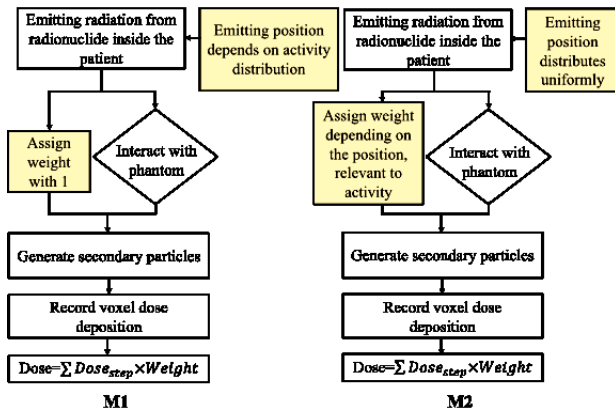


Figure 3. The process of two methods estimating preclinical voxel-based dosimetry.

In Method 3, the mean absorbed doses of each organ were calculated by Monte Carlo simulation with parameters extracted from the same PET/CT images based on MIRd schema for comparison with the results of M1 and M2. In this method, the primary particle was sampled uniformly inside the source organ. The mean absorbed dose ( $D$ ) in the target organ ( $Y_t$ ) was calculated using the equation (2). Activity ( $\tilde{A}$ ) in the source organs ( $Y_s$ ) was obtained from the PET image-based biodistribution data and the S-values( $S(Y_s \rightarrow Y_t)$ ) was calculated by GEANT4.

$$D(Y_s \rightarrow Y_t) = \tilde{A} \times S(Y_s \rightarrow Y_t) \quad (2)$$

**Data processing and dose evaluations**

From the GEANT4 program, the voxel-based three-dimensional distribution of dose rate was obtained. By multiplying the dose rate map and corresponding cumulative activity, the dose was obtained. The data processing and statistics was performed by MATLAB (version R2015b).

In order to quantitatively evaluate the difference of the average absorbed dose calculated by different methods, the parameter of relative difference was defined as equation (3):

$$\text{relative difference} = \frac{D_{M1} - D_{M2}}{D_{M2}} \times 100\% \quad (3)$$

**RESULTS**

**Activity of each organ**

Combined with organ target information, the total

activity of organs at 2 H was shown in figure 4. The results showed that the lung exhibited the highest activity ( $2.4 \times 10^5$  Bq), followed by skeleton ( $2.2 \times 10^5$  Bq), liver ( $2.2 \times 10^5$  Bq), heart ( $1.2 \times 10^5$  Bq), tumor ( $7.3 \times 10^4$  Bq), and kidney ( $2.6 \times 10^4$  Bq).

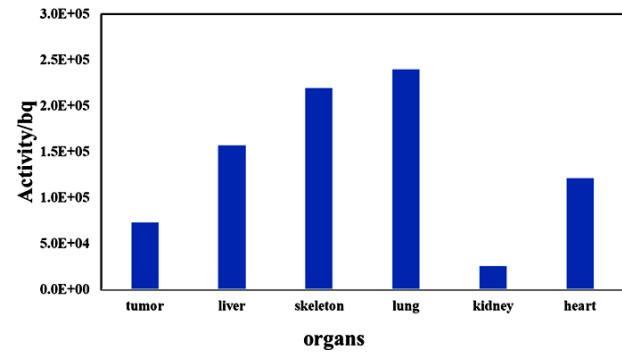


Figure 4. Activity of organs of the mouse at 2 H.

**Average absorbed dose of target organs**

Figure 5 shows the mean dose of the selected organs (i.e. heart, lung, liver, skeleton kidney) and the tumor estimated by GEANT4 MC simulation at 2 H. Among absorbed dose results obtained by M1, the lung exhibited the highest absorbed dose ( $0.0055 \text{ mGy MBq}^{-1}$ ), followed by liver ( $0.0048 \text{ mGy MBq}^{-1}$ ), heart ( $0.0045 \text{ mGy MBq}^{-1}$ ), kidney ( $0.0023 \text{ mGy MBq}^{-1}$ ), tumor ( $0.0021 \text{ mGy MBq}^{-1}$ ) and skeleton ( $0.0019 \text{ mGy MBq}^{-1}$ ). Meanwhile, among absorbed dose results obtained by M2, the liver exhibited the highest absorbed dose ( $0.0051 \text{ mGy MBq}^{-1}$ ), followed by heart ( $0.0050 \text{ mGy MBq}^{-1}$ ), lung ( $0.0049 \text{ mGy MBq}^{-1}$ ), tumor ( $0.0023 \text{ mGy MBq}^{-1}$ ), kidney ( $0.0022 \text{ mGy MBq}^{-1}$ ) and skeleton ( $0.0019 \text{ mGy MBq}^{-1}$ ). Similarly, among the results calculated by M3, the lung illustrated the highest absorbed dose ( $0.013 \text{ mGy MBq}^{-1}$ ), followed by liver ( $0.011 \text{ mGy MBq}^{-1}$ ), heart ( $0.093 \text{ mGy MBq}^{-1}$ ), tumor ( $0.040 \text{ mGy MBq}^{-1}$ ) and skeleton ( $0.021 \text{ mGy MBq}^{-1}$ ).

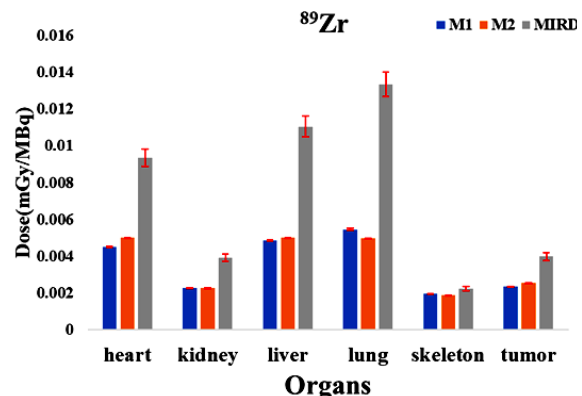


Figure 5. Average absorbed dose of organs obtained by three methods.

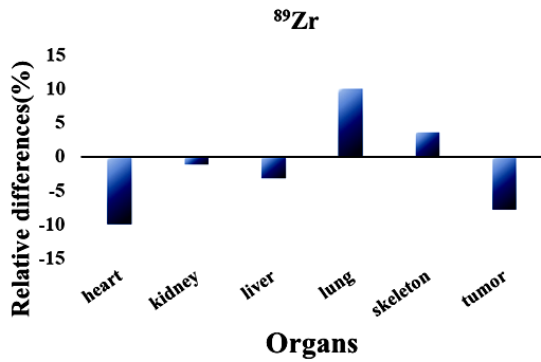


Figure 6. Relative difference between estimated by M1, M2 simulation. The positive values indicate that the absorbed dose values of M1 were larger than those of M2.

As shown in the figure 6, among the percentage differences between M1 and M2, lung illustrates the largest gap (10.00%), followed by heart (-9.97%), tumor (-7.80%), brain (-5.86%), skeleton (3.56%), liver (-3.71%). Kidney illustrates the smallest gap (-1.11%). The average relation difference is 5.9% for all considered organs.

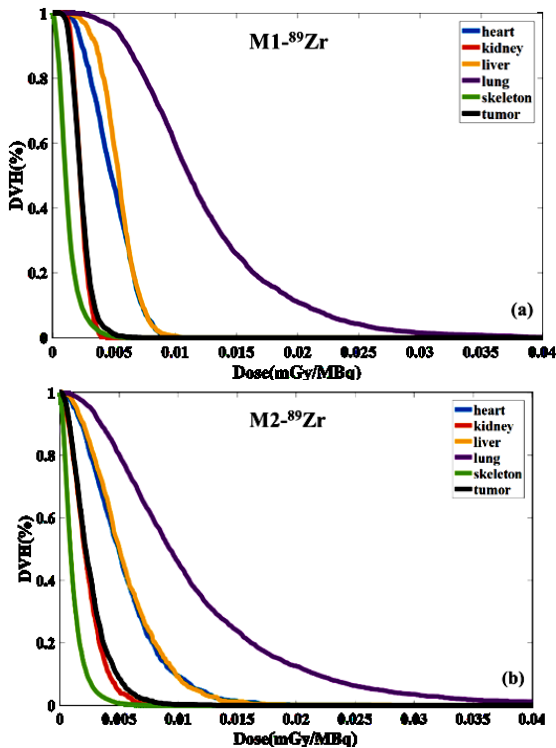


Figure 7. DVH of organs and tumor in the mouse calculated by M1 (a) and M2 (b).

**Three-dimensional dose distribution of target organs**

As shown in figure 7, due to heterogeneous tissue compositions and activity distributions, the dose distribution in the tumor and organs of mouse is uneven, and the degree of unevenness in the lung is the highest, indicating that it is necessary to take

tissue compositions and activity distributions into consideration. Besides, the unevenly distributed three-dimensional dose distribution makes internal dosimetry evaluation and the estimation of the treatment effect of TRT more comprehensive and precise. Furthermore, after obtaining the DVH map, it is possible to calculate the TCP (tumor control probability) and NTCP (normal tissue complication probability) of the internal radiation treatment plan, and evaluate the curative effect from the biological effect rather than the physical dose.

**Calculation time and uncertainties of three methods**

For each simulation, it was repeated 5 times to get the deviation, which is the variance of the average absorbed dose of the target organs and tumor between each simulation result. As is illustrated in the table 1, the average calculation time and result deviation of M2 are the least, with consuming-time 4.8 H and variance of absorbed dose of the tumor and target organs in the mouse less than <0.1%, compared with M1 and M3. Thus, it is obviously that M2 has a significant decline in computational time, making the Monte Carlo simulation more effective.

Table 1. Average Calculation time and uncertainties of three methods.

	M1	M2	M3
Consuming-time	7.2 H	4.8 H	10.9 H
Variance of the mean dose	<1%	<0.1%	<5%

**Application for dose calculation in radionuclide therapy**

The example of using the Monte Carlo simulation for radionuclide therapy in terms of the dosimetry and furthermore the treatment efficacy was presented in the radiopharmaceutical development stage. This result is of course not directly applicable for human patients, but the methods is possible to be used for human patient imaging and therapy. Meanwhile, it is reasonable to show the necessarily of considering animal-specific or patient-specific heterogeneous tissue compositions and activity distributions simultaneously. <sup>177</sup>Lu were taken as the example of the labeled radioisotope as they are the popular labeled radionuclides for treatment in recent years. When the labeled radionuclide is <sup>177</sup>Lu, it was assumed that the biological distribution of radiopharmaceuticals in mice remained similar, which might provide some insights for the radionuclide selection of drug development. The absorbed dose and three-dimensional dose distribution of organs and the tumor in mouse were compared by M1 and M2 while <sup>177</sup>Lu are used as the labeled radionuclides.

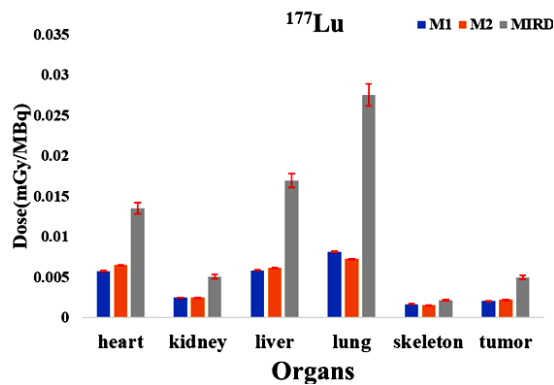


Figure 8. Average absorbed dose of organs obtained by three methods.

Figure 8 illustrated that the average absorbed dose of organs and the tumor calculated by M1 and M2 while the labeling radionuclide is  $^{177}\text{Lu}$  at the same amount of medicine injection. The difference in average absorbed dose calculated by M1 and M2 is generally less than 10%. The consumed simulation time of M1 is 8.2 H, while that of M2 is 4.8 H. The difference in simulation time between M1 and M2 is nearly 41%. As estimated in figure 9, the dose histogram of the organ dose distribution calculated by M1 and M2 is consistent.

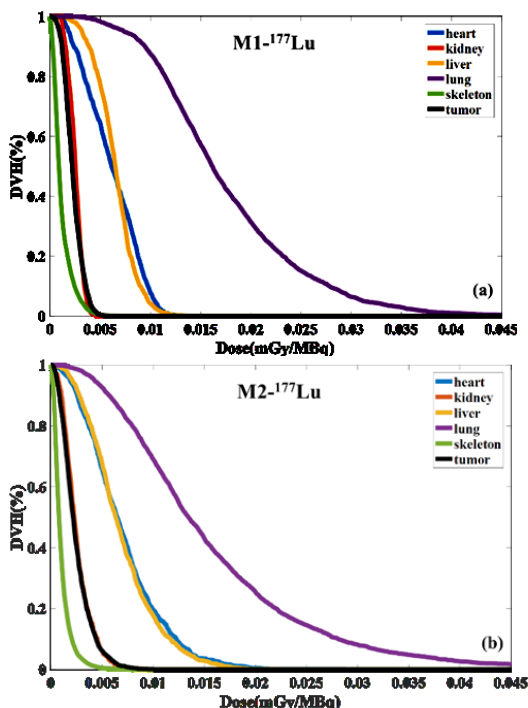


Figure 9. DVH of organs and the tumor in the mouse calculated by M1 (a) and M2 (b) when labeling radionuclides is  $^{177}\text{Lu}$ .

## DISCUSSION

This study aims to investigate voxel-level dose calculation methods in nuclear medicine and propose a new sampling technique, which intends to improve the calculation efficiency of Monte Carlo dose

calculation. As illustrated in table 1, the voxel-level dose calculation method with the new sampling technique (i.e. M2) consumed much less time than the conventional voxel-level dose calculation method (i.e. M1) and reduced the uncertainty of the dose results. The dose results of M1 and M2 are slightly different with imaging radionuclides, which might be mainly due to the statistical error of the Monte Carlo calculation. For radionuclide therapy application, the average absorbed dose result of M2 is still very close to M1, while the simulation time of M2 is 41% less than that of M1 with less deviation. The reduction of time mainly comes from difference of source sampling methods. In traditional methods, the rejection method is often used for source sample which limits the efficiency to some extends<sup>(9,10)</sup>. On the other hand, the uncertainty of dose in the organs with lower activity could be reduced by the uniformed sampling method comparing traditional methods, e.g. M1. The results indicate that the proposed method can be used for efficiency improvement with enough accuracy in voxel-based dosimetry of internal irradiations.

The results also showed that the conventional method based on MIRD formula overestimates the absorbed dose of tumor. Taking a comprehensive look at the differences between M1, M2 and M3 of all cases, the relative difference is 59% and the min absolute value is 12%, showing the huge gap of absorbed dose between the two novel methods estimating preclinical voxel-based dosimetry using PET/CT imaging of mice and traditional MIRD method, manifesting necessity and importance of the consideration into animal-specific or patient-individualized three dimensional tissue and radioactivity distributions<sup>(19, 20)</sup>. Arun Gupta et al. compared the absorbed dose with voxel-level dose calculation for normal mice from  $^{18}\text{F}$ -fluorodeoxyglucose ( $^{18}\text{F}$ -FDG) based on GATE MC simulation and the organ-level dose estimation with image-based dosimetry by MIRD schema<sup>(9)</sup>. The percentage differences is about -22.4% for liver comparing the voxel-based absorbed dose calculated by GATE MC and organ-level estimation by MIRD schema. This is comparable to the result in this work, however, there are differences which comes from different mouse model and drug etc.

However, this study has several limitations. Firstly, although M2 achieved significant improvement in computational efficiency, it still takes several hours, making it difficult to apply in clinic daily practice. For the purpose of reducing the time required for calculation, parallel processing can be used in the future. Also, in recent years, there have been related studies that have introduced artificial intelligence into the prediction of three-dimensional radiation doses<sup>(21)</sup>, greatly reducing the time required for dose assessment. In the next step, we will try to use the internal radiation dose obtained by

M2 as a training sample set, introducing deep learning into the evaluation of the three-dimensional internal radiation dose. Secondly, there were some deviations in the delineation of target organs and tumors, resulting in slightly different dose results. The method of automatically and accurately delineating the target volume also needs further exploration.

## CONCLUSION

Two voxel-based dose calculation methods of radiopharmaceutical internal radiation based on GEANT4 were implemented. A new sampling technique to improve the calculation efficiency of Monte Carlo dose calculation was proposed. The results confirmed the feasibility of the proposed methods and that radiopharmaceutical biodistributions significantly affect the accuracy of internal radiation dose assessment.

## ACKNOWLEDGEMENTS

Not applicable

**Ethics approval and consent to participate:** None.

**Conflict of Interest:** All authors declare no conflict of interest.

**Funding:** National Natural Science Foundation of China (Grant No. 11975123, 11905106); Natural Science Foundation of Jiangsu Province (Grant No. BK20190410); The Foundation of Graduate Innovation Center in NUAA (Grant No. kfjj20190615).

**Authors' contributions:** All authors contributed equally to the design of the study, data collection and analysis, and the writing of the manuscript. All authors read and approved the final manuscript.

## REFERENCES

1. Fahey F, Zukotynski K, Capala J, Knight N (2014) Targeted radionuclide therapy: proceedings of a joint workshop hosted by the National Cancer Institute and the Society of Nuclear Medicine and Molecular Imaging. *Journal of Nuclear Medicine*, **55**(2): 337-348.
2. Kolbert KS, Watson T, Matei C, Xu S, Koutcher JA, Sgouros G (2003) Murine S factors for liver, spleen, and kidney. *Journal of Nuclear Medicine*, **44**(5): 784-791.
3. Boutaleb S, Pouget JP, Hindorf C, Pèlerin A, Barbet J, Kotzki PO, Bardiès M (2009) Impact of mouse model on preclinical dosimetry in targeted radionuclide therapy. *Proceedings of the IEEE*, **97**(12): 2076-2085.
4. Bolch WE, Eckerman KF, Sgouros G, Thomas SR (2009) MIRD pamphlet no. 21: a generalized schema for radiopharmaceutical dosimetry—standardization of nomenclature. *Journal of Nuclear Medicine*, **50**(3): 477-484.
5. Lee MS, Kim JH, Paeng JC, Kang KW, Jeong JM, Lee DS, Lee JS (2018) Whole-body voxel-based personalized dosimetry: the multiple voxel S-value approach for heterogeneous media with nonuniform activity distributions. *Journal of Nuclear Medicine*, **59**(7): 1133-1139.
6. Berger MJ (1971) Distribution of Absorbed Dose Around Point Sources of Electrons and Beta Particles in Water and Other Media. National Bureau of Standards, Washington, DC.
7. Seltzer SM (1991) Electron-photon Monte Carlo calculations: the ETRAN code. *International Journal of Radiation Applications and Instrumentation. Part A. Applied Radiation and Isotopes*, **42**(10): 917-941.
8. Bolch WE, Bouchet LG, Robertson JS, Wessels BW, Siegel JA, Howell RW, Erdi AK, Aydogan B, Costes S, Watson EE, MIRD Committee (1999) MIRD pamphlet no. 17: the dosimetry of nonuniform activity distributions—radionuclide S values at the voxel level. *Journal of Nuclear Medicine*, **40**(1): 115-365.
9. Gupta A, Lee MS, Kim JH, Park S, Park HS, Kim SE, Lee DS, Lee JS (2019) Preclinical voxel-based dosimetry through GATE Monte Carlo simulation using PET/CT imaging of mice. *Physics in Medicine & Biology*, **64**(9): 095007.
10. Silva CC, Berdeguez MB, Barboza T, Souza SA, Braz D, Silva AX, Sa LV (2020) Preclinical radiation internal dosimetry in the development of new radiopharmaceuticals using GATE Monte Carlo simulation. *Radiation Physics and Chemistry*, **173**: 108879.
11. Shirmardi SP, Saniei E, Das T, Noorvand M, Erfani M, Bagheri R (2020) Internal dosimetry studies of <sup>170</sup>Tm-EDTMP complex, as a bone pain palliation agent, in human tissues based on animal data. *Applied Radiation and Isotopes*, **166**: 109396.
12. Auditore L, Amato E, Italiano A, Arce P, Campenni A, Baldari S (2019) Internal dosimetry for TARE therapies by means of GAMOS Monte Carlo simulations. *Physica Medica*, **64**: 245-251.
13. Meftah S, Kraïem T, Elj S, Ben-Ismaïl A (2021) Radioiodine (<sup>131</sup>I) treatment for Graves' disease: Geant4 Monte Carlo simulation for patient personalized dose estimation. *International Journal of Radiation Research*, **19**(1): 213-221.
14. Frezza A, Joachim-Paquet C, Chauvin M, Després P (2020) Validation of irtGPUMCD, a GPU-based Monte Carlo internal dosimetry framework for radionuclide therapy. *Physica Medica*, **73**: 95-104.
15. Masa-Ah P and Soongsathitanon S (2010) A novel standardized uptake value (SUV) calculation of PET DICOM files using MATLAB. in *WSEAS Int Conf on Biomedical Electronics and Biomedical Informatics*, 413-416.
16. Schneider W, Bortfeld T, Schlegel W (2000) Correlation between CT numbers and tissue parameters needed for Monte Carlo simulations of clinical dose distributions. *Physics in Medicine & Biology*, **45**(2): 459.
17. Kikinis R, Pieper SD, Vosburgh KG (2014) 3D Slicer: a platform for subject-specific image analysis, visualization, and clinical support. In *Intraoperative imaging and image-guided therapy*. Springer, New York, NY. 277-289.
18. Asai M, Dotti A, Verderi M, Wright DH, Geant4 Collaboration (2015) Recent developments in Geant4. *Annals of nuclear energy*, **82**: 19-28.
19. Chiesa C, Bardiès M, Zaidi H (2019) Voxel-based dosimetry is superior to mean-absorbed dose approach for establishing dose-effect relationship in targeted radionuclide therapy. *Medical physics*, **46**(12): 5403-5406.
20. Xiao Y, Roncali E, Hobbs R, St James S, Bednarz B, Benedict S, Dewaraja YK, Frey E, Grudzinski J, Sgouros G, Buchsbaum JC (2021) Toward individualized voxel-level dosimetry for radiopharmaceutical therapy. *International Journal of Radiation Oncology, Biology, Physics*, **109**(4): 902-904.
21. Xue S, Gafita A, Afshar-Oromieh A, Eiber M, Rominger A, Shi K (2020) Voxel-wise prediction of post-therapy dosimetry for <sup>177</sup>Lu-PSMA I&T therapy using deep learning. *Journal of Nuclear Medicine*, **61**(1): 1424.